The Visco-Elasto-Plastic Behavior Of Cement Paste At Nanoscale

Nasser Asroun*
Civil Engineering and Environment
Laboratory, Djillali Liabes
University Sidi Bel-Abbes Algeria

Aissa Asroun
Civil Engineering and Environment
Laboratory, Djillali Liabes
University Sidi Bel-Abbes Algeria

Abstract

In presents study, a visco-elasto-plastic material model on the basis of power-law creep relationship was investigated to simulate the indentation load versus depth response of cement paste for one cycle of loading, that including loading, holding and unloading periods. The proposed model through an axisymmetric finite element simulation is able to reproduce the full indentation response and successfully captures the unloading response of cement paste.

Keywords: *nanoindentation; cement Paste; ANSYS; creep; plastic deformation.*

1. Introduction

Current study interest in modeling of behavior of cement paste at nanoscale. Previous studies have shown that cement paste which is the fundamental representative building materials like concrete, exhibits elastic, viscous and plastic strains at nanoindentation tests. It has been modeled recently with analytical solution [1], simplified loading history with loading-holding periods and without intermediate of unloading periods. Indentation has become a standard tool for investigating the small-scale material behavior of most matter such as building materials, polymers, biomaterials and food products. Since most of these materials exhibits time dependent and time independent response, a visco-elasto-plastic material
model is essential for modeling this response. Theoretical studies to characterize the material properties by indentation were first conducted by Hertz, wherein he developed a relationship between the load and indentation depth for elastic bodies [2]. Lee and Radok [3] later extended this theory to viscoelastic bodies by incorporating Boltzmann integral operators to develop a model for spherical indentation. Further extensions were later made to the Lee and Radok model by Ting [4] and Yang [5]. A standard method for obtaining the modulus and hardness of an elastic material by indentation from load-displacement data has been established by Oliver and Pharr [6]. They have developed equations for evaluating the hardness and elastic modulus from indentation load-displacement data.
Nanoscale characterization of cement based materials has shown that nanoindentation is an adequate technique for extracting nanomechanical properties [7]. Moreover, researchers such as Constantinides et al [8] and Mondal et al [9] showed that nanoindentation can be effectively used to extract the mechanical properties of the different phases of Calcium Silica Hydrate (C-S-H) which is the chemical compound responsible of most of the cement paste deformation.
This paper trough the proposed model examines the variation of the indentation depth of cement paste for different times of creeping, different levels of indentation (large or pointed indentation) and different levels of loading. We show that the load-displacement curves gathered during nanoindentation experiments can be modeled successfully using the Finite Element Method (FEM) providing the opportunity to infer a pseudo-continuum behavior of cement paste at the nanoscale.

2. Theory

2.1 Mathematical modeling

Using the Oliver and Pharr method [6](1992), the elastic modulus of the indented sample can be inferred from the initial unloading contact stiffness, $S = dp/dh$, i.e., the slope of the initial portion of the unloading curve, as shown in Figure 1.

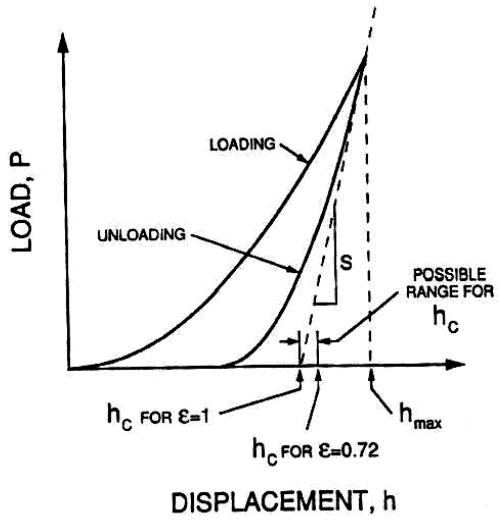

Figure 1: Loading and unloading curve

Based on the relationships developed by Snedden [10] for the indentation of an elastic half space by any punch that can be described as a solid of revolution of a smooth function, a geometry-independent relation involving contact stiffness, contact area, and elastic modulus can be derived as follows:

$$S = 2\beta\sqrt{\frac{A}{\pi}}E_r \quad (1)$$

Whehere β is a constant that depends on the geometry of the indenter. For Berkovich indenter, $\beta = 1.034$ and E_r is the reduced elastic modulus, which accounts for the fact that elastic deformation occurs in both the sample and the indenter. E_r is given by

$$\frac{1}{E_r} = \frac{1-\nu^2}{E} + \frac{1-\nu_i^2}{E_i} \quad (2)$$

Where E and ν are the elastic modulus and Poisson's ratio for the sample, respectively, E_i and ν_i are the same quantities for the indenter. For an indenter with a known geometry, the projected contact area is a function of the contact depth. The area function for a perfect Berkovich indenter is given by

$$A = f(h_c) = 24.56h_c^2 \quad (3)$$

Indenters used in practical nanoindentation testing are not ideally sharp. Therefore, tip geometry calibration or area function calibration is needed. A series of indentations is made on fused quartz at depths of interest. A plot of A versus h_c can be curve fit according to the following functional form

$$A = f(h_c) = 24.56h_c^2 + C_1h_c^1 + C_2h_c^{1/2} + C_3h_c^{1/4} + \cdots + C_8h_c^{1/128} \quad (4)$$

where C_1 to C_8 are constants. The lead term describes a perfect Berkovich indenter.

In case of analytical extraction of elastic properties through nanoindentation data it is possible to assess roughly the yield stress as being directly correlated with hardness value according to Tabor [11], and given by the following equation :

$$\sigma_y \approx H/C \quad (5)$$

where coefficient C can change in the range of 2.6-3.0.

2.2 Finite element modeling

The model consists of the simulation of nanoindentation test of cement paste on 2D planar model using the commercial finite element package ANSYS v.11.0 [12]. A Berkovich diamond indenter were used to perform the indentation test presented in this work. It had a pyramid shape with face angle of 65.27°. For simplicity purposes, the Berkovich indenter is commonly modeled as a conical indenter with a semi-apex angle of 70.3 degrees. This gives the same area to depth function as that of Berkovich indenter. A square area with dimensions including a base of 600 μm, a height of 600 μm was created to represent the cement paste specimens. The indenter and specimen are meshed by 2D structural PLANE182 element as shown in Figure 2.

Nodes along the centerline are constrained to move in *x*-direction and the nodes at the bottom line are constrained to move in *x* and *y*-directions. Axisymmetry conditions are applied along the centerline. The interaction of the indenter and the specimen is modeled as a contact pair with no friction. Contact element TARGET169 is applied to the Berkovich tip and CONTACT172 to the specimen. Load control technique is used to apply different increasing loads at maximum of 0.5 mN, 1 mN, and 2 mN to the upper portion of the indenter in *y*-direction and the displacement in *y*-direction along the upper line of the specimen is measured.

Nanoindentation testing with a sharp pyramidal indenter, such as Berkovich or Vickers, is one of the most complex contact mechanics problems. This is due to the 3 dimensional phenomenon associated with large elastic or elasticplastic deformations. In this case, finite element analysis

trough the approach of large-deformation can provide valuable results to show the displacement and stress distribution of the specimen material during both loading and unloading processes [13]. In the analysis, load applied to the indenter can be force or displacement load. Both of them should be applied in a series of increments. Every step of load should be very small. If this is not the case, the program will not run smoothly.

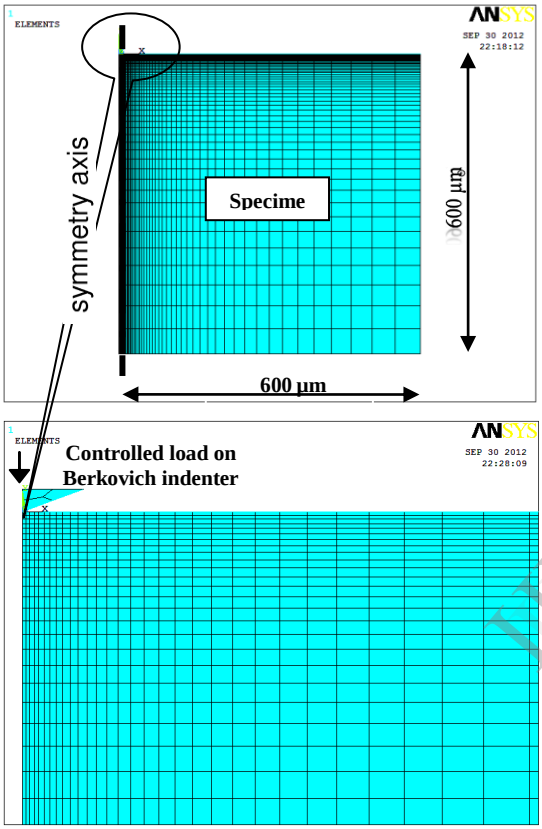

For nanoindentation simulation, large deformation, and geometric considerations must be included in the analysis. To solve these nonlinear large strain problems, maximum number of sub steps cannot be too small. The large strain feature of the ANSYS finite element package was used to simulate the indentation process defined in the model. An updated Lagrangian formulation was adopted in the program due to the large displacements which may arise beneath the indenter during plastic deformation. For the diamond indenter an elastic linear isotropic model with Young modulus E_i =1141 GPa and Poisson ratio ν_i = 0.07 was used. For the cement paste, an elastic perfectly plastic material model with Von Mises yield criterion (σ_y) and Bilinear isotropic time hardening with implicit creep was chosen to extract the creep and plastic strains of the material. Based on published cement properties, the Young's modulus and Poisson's ratio of three types of cement paste (OPC : Ordinary Portland Cement, NVC30 cement paste : Normal Vibrated Concrete class30 cement paste, HD of C-S-H (OPC) : High Density of C-S-H of OPC) were presented in Table 1.

Table 1: Material properties of cement paste

Material	Young's modulus E(GPa)	Initial yield stress σ_y (GPa	Poisson's Ratio ν
OPC[14]	27	0.21[15]	0.24
NVC30[16]	45	0.26	0.25
HD of C-S-H of (OPC)[17]	38.6 ± 2.6	0.5[15]	0.21

The viscous strain may be calculated according to the principle of superposition, summing the strain histories produced by infinitesimal stress increments dσ (t′):

$$\varepsilon(t) = \int_0^t J(t,\hat{t})\,d\sigma(\hat{t}) + \varepsilon_0 \qquad (6)$$

For numerical solution, it is convenient to convert Equation (6) to a rate-type formulation based on Kelvin or Maxwell chain, (see Šmilauer and Bažant, [18]). In the case of the Maxwell model, the material's rate of creep is the summation of elastic strain rate, $(d\sigma/dt)(1/E)$, and viscoelastic strain, σ/η, and is shown as follows:

$$d\varepsilon/dt = (d\sigma/dt)(1/E) + \sigma/\eta$$
$$d\sigma/dt = -\sigma(E/\eta)$$
$$(d\sigma/\sigma) = -(E/\eta)\,dt$$
$$ln\sigma - ln\sigma_0 = -(E/\eta)\,t$$
$$\ln(\sigma/\sigma_0) = -(E/\eta)\,t$$
$$\sigma = \sigma_0 \exp(-Et/\eta) \qquad (7)$$

Equation (7) which is derived from a creep response represents the time dependent change in stress for stress relaxation. From equation (7), it is observed that the slope of the log σ versus time plot is: $-(E/\eta)$ (8)

This information is helpful since the modulus of elasticity, E, can be readily found from a rapidly applied load within the elastic range of the material. The viscosity, η, can then be determined using the slope of the log σ versus time graph. Libraries of creep strain rate equations are included under the "Implicit Creep Equations" sections of ANSYS v.11.0 (user manual ANSYS). The implicit primary

creep equation representing the Maxwell model is represented by the following ANSYS equation:

$$\dot{\varepsilon} = d\varepsilon/dt = c_1 \sigma^{C_2} t^{C_3} e^{-C_4/T} \quad (9)$$

where C_2 and C_3 are constants representing exponents of the time and stress variables. $C_4 = Q/R$, in which Q represents activation energy, R represents Boltzmann's constant, and T represents absolute temperature. For this study, the temperature term is ignored and $-Q/RT$ is zero, making $\exp(-0)$ equal to 1. The three coefficients $C_1, C_2 and C_3$ were determined by fitting procedure of nanoindentation curves shown in Figure 3. Results of the FE simulation were compared with experimental ones by least squares method and the best coefficients were obtained.

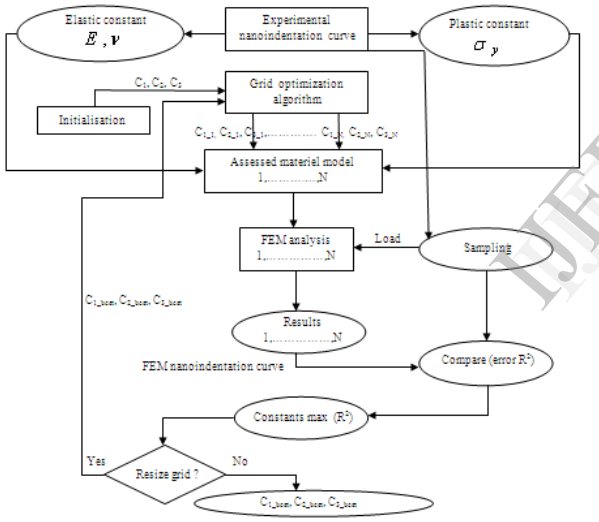

Figure 3: Flowchart of the algorithm for material constants optimization

3. Results and discussion

The simulation results of indentation test of cement paste at nanoscale with the visco-elasto-plastic material model were presented in this section. The indentation depth is shown on X-axis and load on Y-axis. It can be observed that the maximum load of 1 mN obtained against maximum indentation depth of 225 nm and 295 nm is in good agreement with that of the experimental results of Pichler [14] and [19] shown in Figure 4a and Figure 4b.

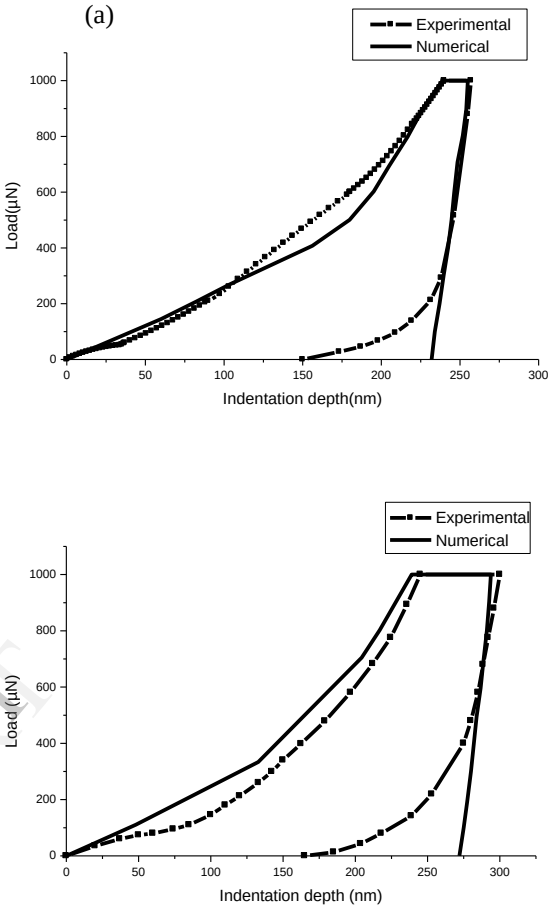

Figure 4: Load-indentation depth curves of OPC for different times of creeping : (a) for 350s, (b) for 400s

It reveals that model is able to capture the viscous strains for various times of creeping (for 350s and 400s).
Similarly, the simulation results of indentation of Ordinary Portland Cement (OPC) with consideration of the size effect are shown in Figure 5a and Figure 5b.

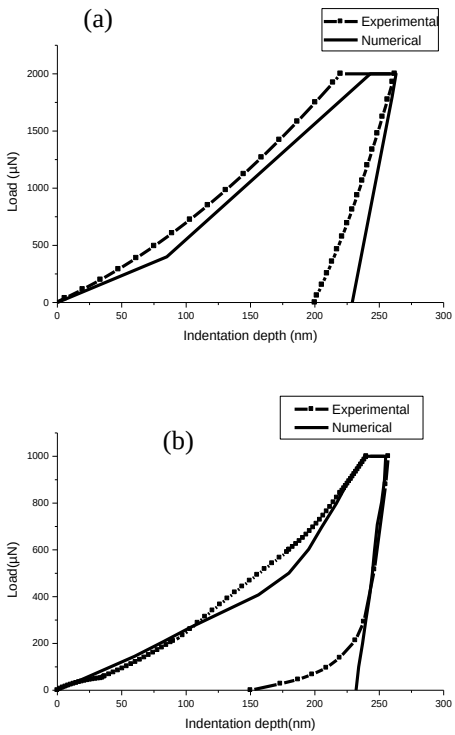

Figure 5: Load-indentation depth curves of OPC for different levels of indentation : (a) for pointed indentation, (b) for large indentation.

In this case also, it can be observed that the results obtained for both levels of indentation : for the pointed indentation of high density of C-S-H and for pointed indentation of high density of C-S-H and for large indentation covering the whole of the phase compound of OPC are quite similar to the experimental results of Nemecek [17] and Pichler [14].

The distribution of Von Mises stress with the maximum displacement of NVC30 cement paste at two levels of loading of 0.5 mN and 1 mN is shown in Figure 6a and Figure 6b.

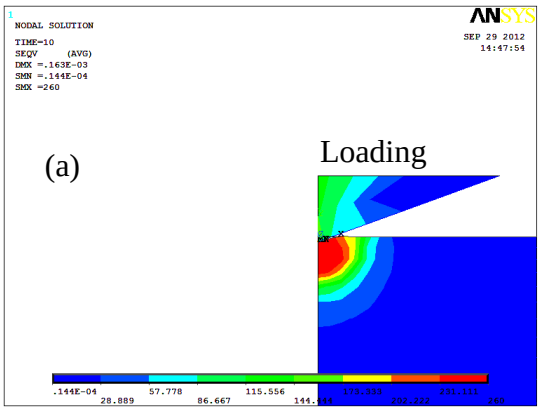

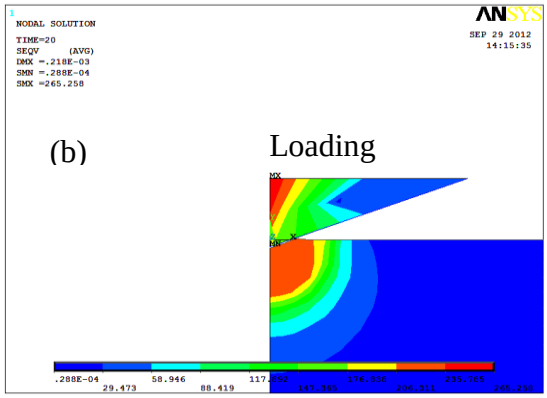

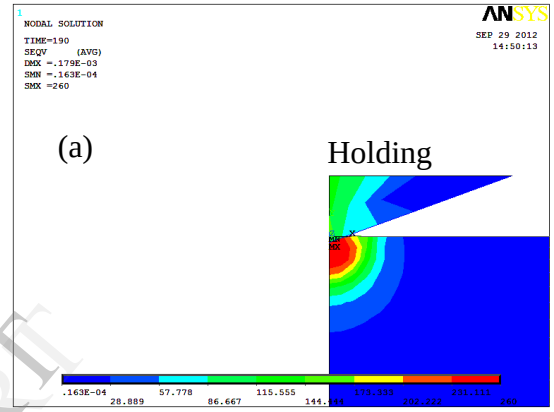

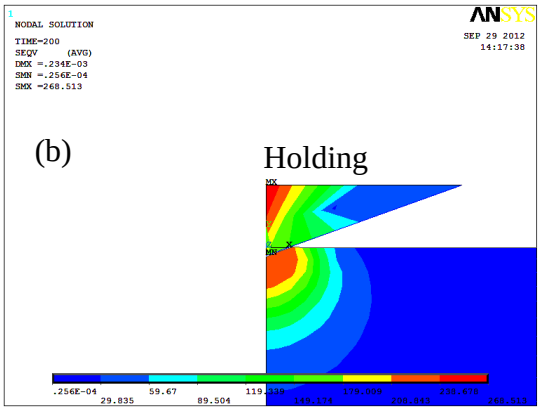

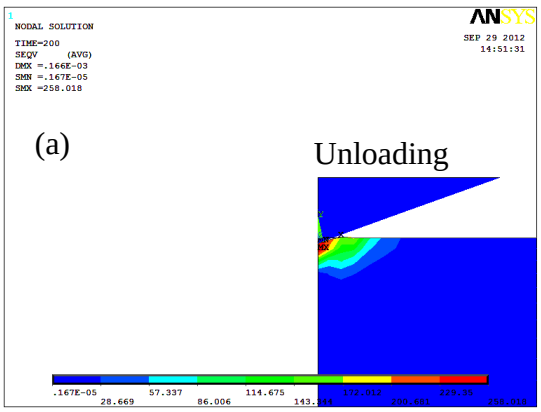

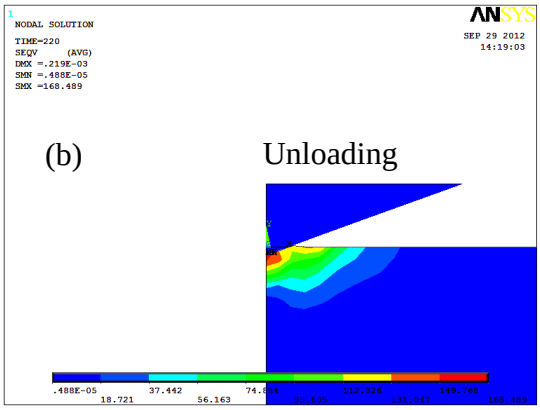

Figure 6: Distribution of Von Mises stress of NVC30 cement paste : (a) for 0.5 mN, (b) for 1 mN.

Greater maximum Von Mises stress-affected zones are found at the maximum level of 1 mN especially for loading and holding steps. However, the stress distribution patterns show no differences from one to another.

In Figure 7, the FEM for two different levels of loading at maximum of 0.5 mN and 1 mN of cement paste of NVC30 was presented.
For both levels of loading, the simulation results are in good correlation with the experimental results presented from Reinhardt [16].
From the nanoindentation experiment, the elastic and plastic constants were directly identified. Remaining constants for the visco-elasto-plastic material model were identified using FEA of the nanoindentation test. Different experimental and numerical curves were dressed to variety of parameters (peak forces, holding times, concrete compositions). Resulting implicit creep constants are shown in Table 2.

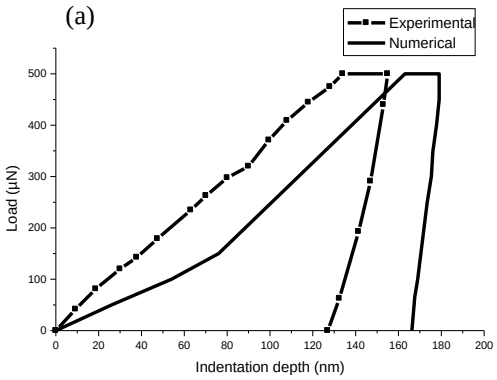

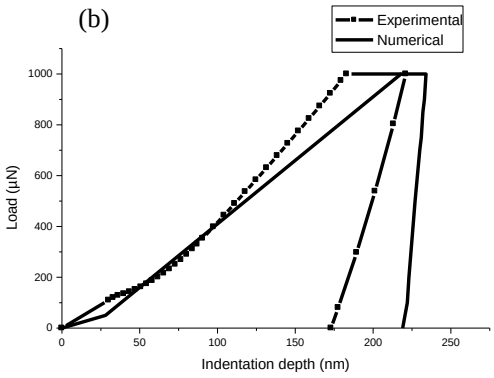

Figure 7: Load-indentation depth curves of NVC30 for different levels of loading: (a) for P_{max}=0.5 mN, (b) for P_{max}=1 mN.

Table 2: Material implicit creep constants for different concrete and cement paste

C_1	C_2	C_3	C_4
$1.3e^{-8}$	1.2	0.15	0
$\pm 0.3e^{-8}$	± 0.2	± 0.05	0

It is evident that some constants have standard deviations which assess in some cases 50%. This deviation may be due to several aspects, e.g: (i) The indentation curves used in FEA were obtained from various indentation matrix of concrete; (ii) the sensitivity of the material model on the resulting constants. The second assumption was treated in this section. From the curves we can make following assumptions: (i) values of C_1 should be varied in range of $(1.3 \pm 0.3)e^{-8}$. Lower values have no effect on the FEM curves; (ii) constant C_2 is useful varied up to 1.4, higher values produced large creep which was not observed during the experiment; (iii) from equation 9 and curves in Figures 4, 5 and 7, it is evident that constant C_3 has significant effect only for values in order to 0.15 ± 0.05. A higher value than this value has not significant influence on the material model; (iv) constant of temperature creep C_4 has zero effect during the FEA and cannot be varied.

According to the above discussion, the load-displacement curves of numerical simulation agree well with the experimental when elastic perfectly plastic properties are adopted in ANSYS.

4. Conclusion

In this study, the response of nanoindentation test of cement paste was simulated by visco-elasto-plastic material model. Different levels of comparison for the indentation test were investigated. The numerical and experimental results are compared, and the following conclusions are obtained :

1. The proposed model is able to reproduce the full indentation response of cement paste at nanoscale including elastic, viscous and plastic strains.
2. The validation of this visco-elasto-plastic model was proved for different times of creeping, different levels of indentation and different levels of loading of cement paste.
3. The load-indentation depth curves of numerical simulation agree well with the experimental curves while the elastic perfectly plastic properties are adopted in ANSYS.

5. Acknowledgement

This work was supported in part by the National Council of Evolution of University Projects of Research of Algeria under Grant number CNEPRU J0402120090080.

6. References

[1] Vandamme M, Ulm F-J., Viscoelastic solutions for conical indentation, International Journal of Solids and Structures, 2006, 43 (10), 3142–3165.

[2] Johnson K.L, Contact Mechanics, Cambridge University Press (England), 1985.

[3] Lee E. and Radok J, The Contact Problem for Viscoelastic Bodies, Journal of Applied Mechanics, 1960, 27 (3), pp 438-444.

[4] Ting, T.C.T., The contact stresses between a rigid indenter and a viscoelastic half space, Journal of Applied Mechanics, 1966, 33 (1), pp 845-854.

[5] Yang, W.H., The contact problem for viscoelastic bodies, Journal of Applied Mechanics, 1966, 33 (1), pp395-401.

[6] Oliver W.C and Pharr G.M, An Improved Technique for Determining Hardness and Elastic Moduli using Load and Displacement Sensing Indentation Experiments, Journal of Materials Research, 1992,7 (6), pp 1564-1583.

[7] Saez de Ibarra, Gaitero Y., Erkizia J.J, and Campillo E., Atomic force microscopy and nanoindentation of cement pastes with nanotube dispersions, Physica Status Solidi (a), 2006,203 (6), pp 1076–1081.

[8] Constantinides G. and Ulm F. J, The effect of two types of C-S-H on the elasticity of cement-based materials: results from nanoindentation and micromechanical modeling, Cement and Concrete Research, 2004, 34 (1), pp 67-80.

[9] Mondal P., Shah S.P., Marks L, Nanoscale Characterization of Cementitious Materials, ACI Materials Journal, 2004,105 (1), pp 174-179.

[10] Sneddon I.N., The Relation Between Load and Penetration in the Axisymmetric Boussinesq Problem for a Punch of Arbitrary Profile, International Journal of Engineering and Science, 1965, 3 (1), p. 47.

[11] Tabor D., A Simple Theory of Static and Dynamic Hardness. Proc. R. Soc. Lond. A, 1948, 192 (1), pp 247–274.

[12] ANSYS, Ansys Reference Manual version 11.0, Available via http://www.ansys.com, 2011.

[13] Chi C., 2-D finite element modeling for nanoindentation and fracture stress analysis, Thesis of Master of Science, 2009.

[14] Pichler Ch. and R. Lackner, Identification of Logarithmic-Type Creep of Calcium-Silicate-Hydrates by Means of Nanoindentation, Journal compilation Blackwell Publishing Ltd Strain, 2009, 45 (1), pp 17-25.

[15] Kaushal K. J., Nakin S., Debrupa L. and Agarwal A, Energy-Based Analysis of Nanoindentation Curves for Cementitious Materials, ACI Materials Journal, 2012, 109 (1), pp 81-90.

[16] Reinhardt A, Macro and Nanoscale Creep of Self-Consolidating Concrete, Thesis of Master of Science, 2010.

[17] Nemecek J, Local Micromechanical Properties of Cement Pastes, Chemical Listy, 2011,105 (1), pp 120-122.

[18] Šmilauer V. and Bažant Z.P., Identification of viscoelastic C-S-H behavior in mature cement paste by FFT-based homogenization method, Cement and Concrete Research, 2010,40 (1), pp 197-207.

[19] Pichler Ch., Jager A., Lackner R. and Eberhardsteiner J, 22nd Danubia-Adria Symposium on Experimental Methods in Solid Mechanics, 2005.